8.5
Sonocatalysis

Kenneth S. Suslick and Sara E. Skrabalak*

8.5.1
Introduction and the Origins of Sonochemistry

Research on the chemical effects of ultrasound has undergone a renaissance during the past few decades and has had a significant impact in a variety of areas [1, 2]. Applications of sonochemistry have been developed in virtually all areas of chemistry and related chemical and materials technologies [3–5]. We can conceptually divide the effects of ultrasonic irradiation on heterogeneous catalysis into those that alter the formation of heterogeneous catalysts, those that perturb the properties of previously formed catalysts and those that affect catalyst reactivity during catalysis. In practice, these three classes of effects are often deeply intertwined in reported experimental results.

No direct coupling of the acoustic field with chemical species on a molecular level can account for sonochemistry. Ultrasound spans frequencies from roughly 20 kHz to 10 MHz, with associated acoustic wavelengths in liquids of roughly 100–0.15 mm: these are not on the scale of molecular dimensions. Instead, the chemical effects of ultrasound derive from several non-linear acoustic phenomena, of which cavitation is the most important. Acoustic cavitation is the formation, growth and implosive collapse of bubbles in a liquid irradiated with sound or ultrasound. When sound passes through a liquid, it consists of expansion (negative pressure) waves and compression (positive pressure) waves. These cause bubbles (which are filled with both solvent and solute vapor as well as dissolved gases) to grow and recompress. Under proper conditions, acoustic cavitation can lead to implosive compression in such cavities, producing intense local heating, high pressures and very short lifetimes. As discussed elsewhere, these hot spots have temperatures of roughly 5000 °C, pressures of about 1000 atm (1 atm = 101.325 kPa) and heating and cooling rates above 10^9 K s^{-1} [6–10]. Cavitation is an extraordinary method of concentrating the diffuse energy of sound into a chemically usable form.

References see page 2015

* Corresponding author.

When a liquid–solid interface is subjected to ultrasound, cavitation still occurs, but with major changes in the nature of the bubble collapse. If the surface is significantly larger than the cavitating bubble (~100 μm at 20 kHz), spherical implosion of the cavity no longer occurs, but instead there is a markedly asymmetric collapse which generates a jet of liquid directed at the surface, as seen directly in high speed micro-cinematographic sequences shown in Fig. 1. The tip jet velocities have been measured by Lauterborn to be greater than 100 m s^{-1} [11]. The origin of this jet formation is essentially a shaped-charge effect: the rate of collapse is proportional to the local radius of curvature. As collapse of a bubble near a surface begins, it does so with a slight elliptical asymmetry, which is self-reinforcing and generates the observed jet. The impingement of this jet can create localized erosion (and even melting), surface pitting and ultrasonic cleaning. A second contribution to erosion created by cavitation involves the impact of shock waves generated by cavitational collapse. The magnitude of such shock waves is thought to be as high as 10^4 atmospheres, which will easily produce plastic deformation of malleable metals [12]. The relative importance of these two effects depends heavily on the specific system under consideration.

Enhanced chemical reactivity of solid surfaces is associated with these processes. Cavitational erosion generates unpassivated, highly reactive surfaces; it causes short-lived high temperatures and pressures at the surface; it produces surface defects and deformations; it forms fines and increases the surface area of friable solid supports and it ejects material in unknown form into solution. Finally, local turbulent flow associated with acoustic streaming improves mass transport between the liquid phase and the surface, thus increasing observed reaction rates. In general, all of these effects are likely to be occurring simultaneously.

In contrast, the effects of ultrasound on slurries of fine particles do not come from microjet formation during cavitation. Distortion of bubble collapse requires a solid surface several times larger than the resonance bubble size. Thus, for ultrasonic frequencies of ~20 kHz, damage associated with jet formation cannot occur for solid particles smaller than ~200 μm. In these cases, however, shockwaves created by homogeneous cavitation can create high velocity interparticle collisions, with impact speeds of several hundred meters per second and local effective transient impact temperatures of roughly 3000 K [13, 14]. The turbulent flow and shockwaves produced by intense ultrasound can drive metal particles together at sufficiently high speeds to induce effective melting at the point of collision, as shown in Fig. 2. The high-velocity interparticle collisions produced in slurries of malleable materials cause smoothing of individual particles and agglomeration of particles into extended aggregates [5, 15]. Surface composition depth profiles of sonicated powders show that ultrasonic irradiation effectively removes surface oxide coatings. The removal of such passivating coatings dramatically improves reaction rates for a wide variety of reactions. With larger flakes of brittle materials, interparticle collisions cause shock

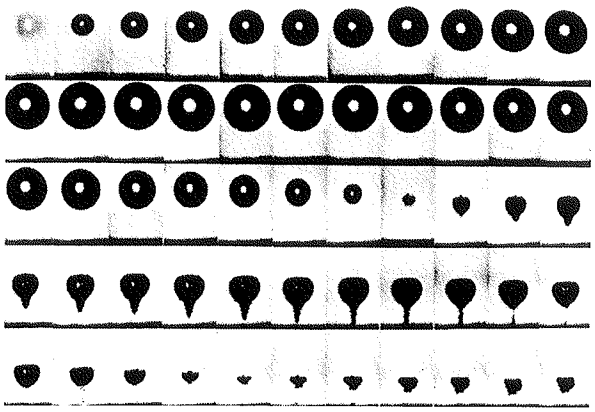

Fig. 1 Cavitation near a liquid–solid interface. High-speed micro-cinematographic sequence of laser-induced cavitation near a solid surface, showing the formation of a microjet impact; 75 000 frames s^{-1}. The sequence is from left to right, top to bottom; the solid boundary is at the bottom of each frame. Photograph courtesy of W. Lauterborn; reproduced with permission [11].

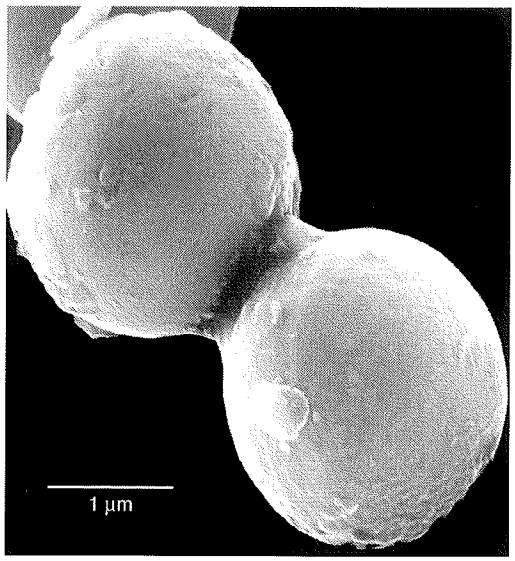

Fig. 2 Scanning electron micrograph of 5 μm diameter Zn powder after ultrasonic irradiation of a slurry in decane. Neck formation from localized melting is caused by high-velocity interparticle collisions. Similar micrographs and elemental composition maps (by Auger electron spectroscopy) of other metal powders and mixed metal collisions have also been made. Reproduced with permission [25].

fragmentation instead, which can increase surface areas dramatically and contribute to increased activity [15–17].

The term *sonocatalysis* should be restricted in its use to refer only to the creation of a catalytically competent intermediate by ultrasonic irradiation. One should *not* refer to a simple sonochemical rate enhancement of a reaction by this term, just as one would use the term photochemistry and not photocatalysis, to describe a stoichiometric reaction caused by light. In this chapter, the symbol shown in Eq. (1) will be used to indicate ultrasonic irradiation or "sonication" of a solution leading to a sonochemical reaction.

$$\xrightarrow{)))} \qquad (1)$$

8.5.2 Effects of Ultrasound on Heterogeneous Catalysts

Ultrasonic irradiation can alter the reactivity observed during the heterogeneous catalysis of a variety of reactions [5, 18]. In addition to the more recent work described in this chapter, there is extensive (but little recognized) past literature in this area, particularly from Eastern Europe [19].

The effects of ultrasound on catalyst formation can be far reaching; changes in crystallization, dispersion and surface properties are all possible. Alteration of properties of pre-formed catalysts can also have substantial effects. Oxide or other passivating coatings can be removed and increased dispersion can occur, sometimes from the fracture of friable supports. Irradiating operating catalysts often improves mass transport.

8.5.2.1 Metal Powders

The use of ultrasound for syntheses involving liquid–solid heterogeneous reactions has been a matter of intense investigation [20–22]. In general, ultrasonic treatment of these metals promotes reaction pathways favoring single electron transfers [23], probably through the removal of thin oxide coatings which are often dominated by acid–base activity. Ultrasonic activation of commercial transition metal powders has also received substantial attention [24–27].

8.5.2.1.1 Modification of Bulk Metals The effect of ultrasonic irradiation on bulk metals has been studied extensively [28–30]. In particular, ultrasonic pretreatment on hydrogenation catalysts has been studied and impressive rate accelerations have been reported. The hydrogenation of alkenes by ordinary Ni powder is enormously enhanced ($>10^5$-fold) by ultrasonic irradiation [24]. The surface area of the catalyst, however, did not change significantly even after lengthy irradiation. Rather, both surface smoothing (Fig. 3) and particle agglomeration were observed, due to interparticle collisions caused by cavitation-induced shock waves. Auger electron spectroscopy revealed a decrease in the thickness of the oxide coat after ultrasonic irradiation; the removal of this passivating layer is likely responsible for the increased catalytic activity.

Ultrasonic treatment of Raney Ni enhances hydrogenation and hydrogen–deuterium exchange rates [31]. Hydrogen isotopes have been selectively introduced into aromatic compounds by the reaction of haloaromatic compounds with basic deuterated (or tritiated) aqueous solutions over Raney catalysts under ultrasound. Carbohydrates and glycosphingolipids have also been deuterated [32, 33]. Treatment of ultrasonically prepared Raney nickel with tartaric acid results in a highly efficient enantioselective catalyst for the hydrogenation of 1,3-diketones to 1,3-diols [34] with a similar catalyst preparatory method having recently been patented [35]. Ultrasound is also being used to regenerate Raney Ni catalysts *in situ* [36, 37].

References see page 2015

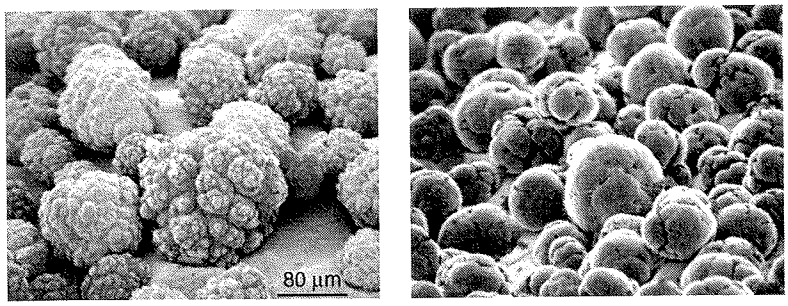

Fig. 3 The effect of ultrasonic irradiation on the surface morphology and particle size of Ni powder. Initial particle diameters before ultrasound were ~160 µm; after ultrasound, ~80 µm; the micrographs are on the same scale. High-velocity interparticle collisions caused by ultrasonic irradiation of slurries are responsible for the smoothing and removal of passivating oxide coating. Reproduced with permission [15].

As an extension of the Raney Ni work, Boudjouk prepared an efficient, recyclable Ni hydrosilation catalyst from the reduction of NiI_2 with Li under ultrasound [38, 39]. The reaction of acrylonitrile had yields >95% at 0 °C, whereas commercial Ni powder was not active even after extensive sonication. More recent work has looked at the hydrogenation of α, β-unsaturated ketones with high yields and chemoselectivity [40].

Ultrasound also influences the properties of platinum and palladium blacks prepared by the reduction of H_2PtCl_6 or $PdCl_2$ in formaldehyde [41]. For Pt black, slight increases in hex-1-ene hydrogenation and ethanol oxidation were observed and explained by an increase in surface area. H_2O_2 decomposition rates, however, were much greater than the corresponding surface area enhancement, suggesting that the amorphous phase generated from ultrasonic irradiation supports H_2O_2 decomposition whereas the hydrogenation and oxidation reactions require more ordered structures not abundantly formed under such conditions.

The allylation of ketones and aldehydes by allylic alcohols [Eq. (2)] has been improved using ultrasonic irradiation of a palladium–tin dichloride catalyst in less polar solvents [42]. Inverted regioselectivity was observed compared with homogeneous carbonyl allylation in polar solvents.

$$H_3CCH{=}CHCH_2OH + H_5C_6CHO \xrightarrow[Pd/SnCl_2]{)))} H_3CCH{=}CHCH_2CH(OH)C_6H_5 \qquad (2)$$

Ultrasound has also been used to prepare Fischer–Tropsch catalysts. Liquid-phase hydrogenation of carbon monoxide was accomplished with ultrafine particles (<100 nm) composed of iron, cobalt and nickel prepared by vapor-phase reduction of metal chlorides and passivated by gradual oxidation [43, 44]. The catalysts initially showed high catalytic activity and oxygenate selectivity. During reaction, however, catalyst degradation occurred due to aggregation. Ultrasonic irradiation regenerated the catalyst. In addition, ultrasonically prepared colloidal K was used to modify the ultrafine particle catalysts, increasing the yield of high molecular weight products. Kikuchi and Itoh [45] examined the Fischer–Tropsch reaction from iron ultrafine particle catalysts (40–80 nm) suspended in hexadecane. Pretreatment with ultrasound increased catalyst activity five-fold compared with the precipitated powder. With these systems, ultrasonic irradiation is apparently used to create dispersions of the weakly aggregating ultrafine particles; this also appears to be the function of ultrasound in the preparation of zeolite (HZSM-5)-supported ultrafine iron particle catalysts, where the activity was increased by a factor of ~20 compared with catalysts made with rapid stirring [46].

8.5.2.1.2 Amorphous and Nanostructured Metal Catalysts

Suslick and coworkers produced amorphous iron, consisting of coral-like agglomerations of a few nanometer-sized clusters (Fig. 4) from the sonolysis of $Fe(CO)_5$ [47–49]. Amorphous metallic alloys lack long-range crystalline order and have unique electronic, magnetic and catalytic properties. The production of amorphous metals is difficult because extremely rapid cooling ($>10^6$ K s^{-1}) of molten metals is necessary to prevent crystallization. Acoustic cavitation can induce extraordinary local heating in otherwise cold liquids and can provide enormous cooling rates ($>10^9$ K s^{-1}), thus providing a new synthetic route to amorphous metal powders. From work on the sonolysis of volatile Co, Mo and W precursors [50], it appears that this is a general phenomenon and extension to the synthesis of amorphous intermetallic alloys has proven successful.

Sonochemically synthesized amorphous powders may have important catalytic applications, especially given their very high surface areas and nanometer cluster size. For example, sonochemically prepared nanophase iron is an active catalyst for the Fischer–Tropsch hydrogenation of CO and for hydrogenolysis and dehydrogenation of alkanes, in large part due to its high surface area (>120 m g^{-1}). Rates of conversion of CO and H_2 to low molecular weight alkanes were approximately 20 times higher per gram of Fe than for fine particle (5 μm diameter) commercial iron powder at 250 °C and more than 100 times more active at 200 °C. Selectivities are similar. The reactions of cyclohexane are interesting because of their inherent catalyst surface-structure sensitivity. In this manner, the nature of the catalytic process can be useful as a chemical probe of

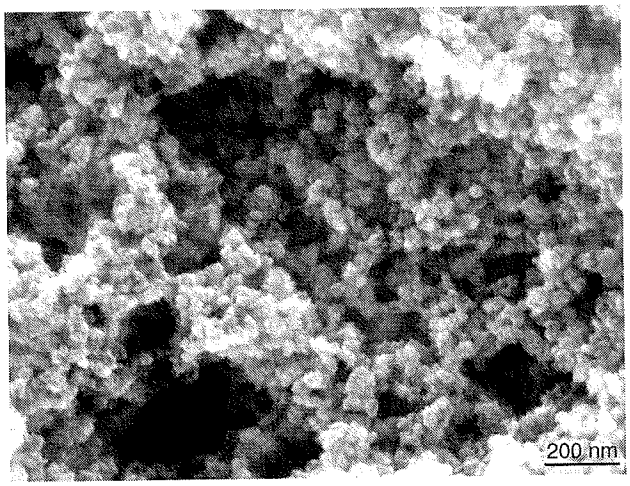

Fig. 4 Scanning electron micrograph of amorphous nanostructured iron powder produced from the ultrasonic irradiation of $Fe(CO)_5$. Reproduced with permission [47].

the effect of ultrasound on the catalytically active surface. Catalytic studies were performed on nanophase Fe/Co alloys produced sonochemically. The ratio of cyclohexane dehydrogenation to hydrogenolysis depended on alloy composition. The 1:1 alloys gave nearly exclusively benzene, in stark contrast to either pure metal [51]. Building on this work, Gedankan and coworkers have looked at the aerobic oxidation of cycloalkanes with Fe, Co and Fe/Ni alloys produced sonochemically [52]; with cyclohexane as a substrate, conversions of 40%, with 80% selectivity for cyclohexanone and cyclohexanol, were achieved under mild conditions.

Several groups have reported the sonochemical synthesis of metal (Cu, Pt, Pd, Au) or bimetallic (Au/Pt, Au/Pd, Co/Ni) nanoparticles; increased rates of hydrogenation for 4-pentenoic acid with Au/Pd catalysts [53] and the Ullman reaction for Cu nanoparticles [54] have been reported. Otherwise, applications of sonochemically generated discrete metallic nanoparticles to catalysis are scant.

8.5.2.2 Metal Oxides as Catalysts

There are many reports on the effects of ultrasound on metal oxide catalyst preparation [55]. Mixed Cr–Mo and Cr–Fe oxide catalysts have been prepared with ultrasonic treatment and examined for the oxidation of methanol to formaldehyde [56, 57]. CuO catalysts were prepared with ultrasound and tested them for de-NO_x reduction [58]. Mokryi and Starchevskii examined the vapor-phase oxidation of a number of organic compounds after ultrasonic activation of Fe–Te–Mo and Cs–Pb–Mo oxide catalysts [59]. Isobutylene, methanol and ethanol were examined; modest increases in specific surface areas and catalytic activity were obtained, but selectivity towards the desired products decreased.

Gedankan and coworkers have published numerous papers on the sonochemical synthesis and catalytic properties of metal oxides. Mesoporous cobalt, nickel and iron oxides have been prepared by incorporating structure-directing agents such as cetyltrimethylammonium bromide (CTAB) in an inorganic precursor solution. Ultrasonic irradiation was supplied under air [60, 61]. After solvent extraction, high surface area materials (α-Fe_2O_3 274, Co_3O_4 72.83, NiO 39.84 $m^2\ g^{-1}$) were produced. Slightly better conversions of cyclohexane to cyclohexanone and cyclohexanol were observed for the calcined oxides compared with other nanostructured forms of the corresponding metal oxides, with the best conversions, ~40%, being obtained for the sonochemically produced Fe_2O_3. The same metal oxides have also been deposited into the pores of mesoporous oxide carriers [62, 63] and incorporated into composites [64] of traditional support materials; the conversions and selectivities were comparable to those for unsupported, sonochemically generated bulk materials. Sahle-Demessie and coworkers have reported selective hydrocarbon oxidation using sonochemically generated vanadium phosphorus oxide (VPO) [65].

It is well known that alumina itself, acting as a solid acid or base, can be an active catalyst for a variety of organic reactions. Early work in this area was conducted by Ando's group [66]. Their initial discovery was the improvement made by ultrasonic irradiation of the liquid–solid two-phase synthesis of aromatic acyl cyanides from acid chlorides and solid KCN in acetonitrile [67]. The extension of this reaction to benzyl bromides led to an unusual observation of reaction pathway switching [68]. With mechanical agitation (i.e. stirring), the reaction of benzyl bromide and KCN in aromatic solvents, catalyzed by alumina, yields diarylmethane products from Friedel–Crafts attack on the solvent [Eq. (3)], whereas with ultrasonic irradiation, one obtains benzyl cyanide [Eq. (4)]. Apparently, the ultrasonic irradiation of alumina deactivates the Lewis acid sites normally present that are responsible for the Friedel–Crafts reactivity. It is thought that this poisoning is accomplished by the added solid basic salts (e.g. KCN) with ultrasound, perhaps through solid–solid contacts or through increased access of dissolved bases to the alumina surface.

$$C_6H_5CH_2Br + C_6H_5CH_3 + KCN \xrightarrow[Al_2O_3]{\text{stirred}} C_6H_5CH_2C_6H_4CH_3 \quad (3)$$

$$C_6H_5CH_2Br + C_6H_5CH_3 + KCN \xrightarrow[Al_2O_3]{)))} C_6H_5CH_2CN \quad (4)$$

Catalysis by alumina in the presence of ultrasound is a generalizable class of reactions, e.g. the sonocatalysis of aldol condensations and related reactions, Michael additions [69, 70] and Knoevenagel condensations [71]. Substantial improvements in yields were observed, with greatly diminished reaction times, for a variety of substrates. In the same vein, a useful synthesis of α-aminonitriles, which are important intermediates in amino acid synthesis, has been reported using alumina with ultrasound [72].

Yu et al. studied the effect of ultrasound on the synthesis and resulting photocatalytic activity of titania. They found that ultrasonic treatment of titania sols accelerated the hydrolysis and crystallization of titania [73]. The dried gels had an increased brookite to anatase ratio compared with titania sols prepared without ultrasound treatment; they also showed a modest increase in photocatalytic activity compared with that of the standard Degussa P25 titania.

References see page 2015

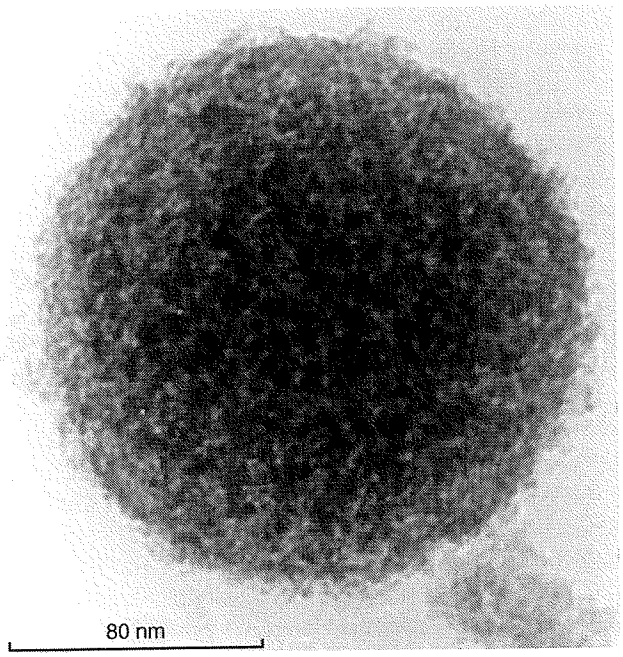

Fig. 5 Transmission electron micrograph of mesoporous titania with a wormhole-like internal structure prepared with high intensity ultrasound. Photograph courtesy of J. Yu; reproduced with permission [74].

Similarly, they found that dropwise addition of titanium isopropoxide–glacial acetic acid–ethanol solution to water under high intensity ultrasonic irradiation generated thermally stable, mesoporous TiO_2 with an unusual wormhole-like structure (Fig. 5) [74]; they attributed this structure to the controlled condensation and agglomeration of TiO_2 sol particles unique to ultrasound irradiation. Calcination resulted in a completely anatase phase TiO_2 network; its photocatalytic activity was found to be slightly greater than that of Degussa P25 titania, probably due to increased surface area and enhanced diffusion of reactants and products. Variations on these procedures are published with similar results [75, 76]. A few reports on the "sonophotocatalytic" properties of titania have also been reported in which cooperative effects between irradiation with sound and light increase the degree of water splitting observed over commercial titania [77, 78].

8.5.2.3 Metal Carbides and Sulfides

Molybdenum and tungsten carbides have been examined as catalysts because their activity is often similar to that of the platinum group metals. For catalytic applications, high surface area materials are needed, but the preparation of molybdenum and tungsten carbides with high surface areas has proven difficult. Suslick and coworkers have synthesized high surface area forms of these carbides [79, 80] from ultrasonic irradiation of $Mo(CO)_6$ or $W(CO)_6$ in hexadecane under an argon atmosphere. Surface areas of 188 $m^2\ g^{-1}$ for Mo_2C and 120 $m^2\ g^{-1}$ for W_2C were obtained. Carburization of the resulting materials induced crystallization and the surface areas decreased slightly to 130 and 60 $m^2\ g^{-1}$, respectively.

The suppression of hydrocracking during dehydrogenation remains a significant challenge for non-platinum catalysts. Sonochemically generated Mo_2C was tested for the dehydrogenation of cyclohexane [79] and found to be highly selective for benzene. In fact, like platinum, no hydrogenolysis products were observed. The overall activity of the sonochemical Mo_2C was comparable to that of Pt.

Sonochemically generated Mo_2C and W_2C were also tested for the hydrodehalogenation (HDH) of monohalobenzenes [80]. Previous studies have emphasized the possibility of using noble metals (primarily Pd, Pt and Rh) for HDH but the use of such metals has been unsatisfactory, as hydrogenation tends to be favored over HDH. Both sonochemically generated Mo_2C and W_2C demonstrated high selectivity for the HDH of monohalobenzenes. For example, no chlorocyclohexane and cyclohexane were observed for the HDH of chlorobenzene. A previous study with conventional Mo_2C reported the hydrogenation of benzene to cyclohexane. The sonochemically generated carbides were also active for the HDH of CFCs, PCBs and their brominated analogs.

Sonochemically generated Mo_2C was also tested for the catalytic hydrodenitrogenation (HDN) of indole [81], a common organonitrogen compound in crude oil. From 300 to 400 °C, slightly higher conversions of indole to aryl amines and hydrocarbons were obtained compared with standards; this result was attributed to more randomly distributed crystallites, a direct consequence of the sonochemical synthesis. Above 400 °C, substantial sintering of the sonochemically generated Mo_2C resulted in a drop in activity below that of the standards.

Given the increasingly strict regulation of the sulfur content of fuels, improved hydrodesulfurization (HDS) catalysts are needed. Molybdenum sulfide is traditionally used; however, as HDS activity is due only to the edges of this layered material, the preparatory method greatly affects its catalytic performance. High-intensity ultrasonic irradiation of $Mo(CO)_6$ and sulfur in isodurene under argon yields nanostructured MoS_2 with a very high edge content [82]. TEM images (Fig. 6) show highly disordered MoS_2 with much greater edge and defect content. This MoS_2 was tested for the HDS of thiophene at atmospheric pressure and found to be highly active: three times more active than conventional MoS_2 at 375 °C and also more active than ReS_2 and RuS_2. Recently, Mo_2N [83], hollow MoS_2 nanospheres [84] and MoS_2 microspheres [85] have also been prepared by ultrasound; the last two both display a higher degree of disorder with higher edge surface

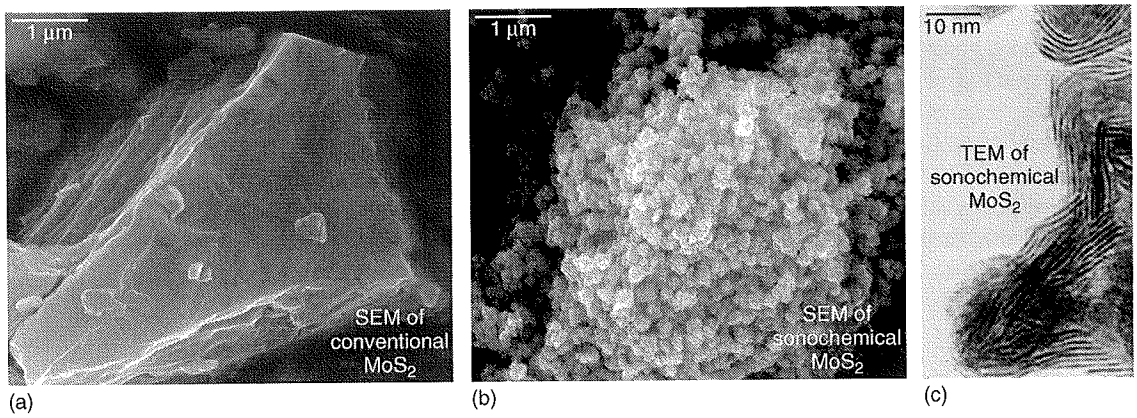

Fig. 6 Scanning electron micrograph of conventional molybdenum sulfide (a) compared with the SEM (b) and TEM (c) of nanostructured MoS_2 produced from the ultrasonic irradiation of $Mo(CO)_6$ and elemental sulfur as a slurry in isodurene. Reproduced with permission [82].

exposure than conventional MoS_2 and enhanced HDS activities.

8.5.2.4 Catalyst Supports: Sonogels and Zeolites

Support materials are used to disperse catalytically active phases. There has been a flurry of research studying the effect that ultrasound has on the synthesis and activation of catalyst support materials. Inorganic supports such as SiO_2 and TiO_2 are typically produced via sol–gel processing. In 1984, Tarasevich described an approach to sol–gel processing that eliminated the need for additional solvent and reduced the preparation time by exposing a gel precursor solution to intense ultrasonic irradiation [86]. Since then, the groups of Esquivias [87] and Zarzycki [88] have studied extensively the effect that ultrasound has on the kinetics and morphology of the resulting "sonogels". The term "sonogel" refers to either a solvent-containing gel or a gas-containing gel (a xerogel) made in the presence of ultrasound. SiO_2, TiO_2, SiO_2-TiO_2, $SiO_2-Al_2O_3-MgO$, $SiO_2-P_2O_5$ and ZrO_2 sonogels have been synthesized [87] and also ormosils (ORganically MOdified SILicates) [89]. The sonogels, upon solvent removal, appear to have finer porosity and greater reticulation of the network than gels prepared without ultrasound. Interestingly, chemical characterization of TiO_2-SiO_2 sonogels showed improved dispersion of Ti in the SiO_2 network [90]. Likewise, a patent was issued for a sonochemical process for preparing Zr containing aluminoxanes [91]. Upon sonication of a toluene solution of $(CH_3)_3Al$ and Cp_2ZrCl_2 with water (Cp = cyclpentadienyl), an aluminoxane gel was formed that was an active catalyst for oligomerization of 1-octene.

Rhodium metal has been dispersed on TiO_2-SiO_2 aerogels [92]. Ultrasound was utilized in two different preparations. In the first case, a "sonogel" was obtained by hydrolysis of Ti and Si alkoxides in the presence of ultrasonic irradiation, which was then impregnated with a rhodium nitrate solution. In the second, a mixture of the alkoxides and a rhodium nitrate solution were exposed to ultrasound, thus leading to a ternary $Rh-TiO_2-SiO_2$ sonogel. The behavior of these catalysts was compared with that of an Rh/TiO_2-SiO_2 system obtained by conventional impregnation methods, starting with a commercial silica support. The first example gave a ca. 10-fold increase in catalytic activity for the hydrogenation of benzene whereas the second sample was not active for benzene hydrogenation due to poor Rh dispersion. Other metals have also been dispersed on to sonogel carriers, with similar results being obtained [90, 92, 93].

Carbon sonogels have been produced by Tamon's group [94, 95]. Irradiation with high-intensity ultrasound promotes the sol–gel polycondensation of resorcinol and formaldehyde, typical precursors for carbon supports. As with the oxides, gelation occurs more rapidly when exposed to ultrasonic irradiation. The resulting carbon gels have increased mesoporosity compared with those prepared without ultrasound and moderate surface areas ($500-800\ m^2\ g^{-1}$). Such materials could be ideal supports for Pt-based fuel cell catalysts.

Ordered, mesoporous SiO_2 structures such as MCM-41 have been prepared via ultrasound with a drastic reduction in fabrication time being reported, down from several days to 3–6 h [96]. The resulting product has thicker pore walls, improving its thermal stability. Although some investigations of the effects of ultrasound on aluminosilicates and their syntheses have been published, this area still remains relatively unexplored. The best characterized study is that of Lindley [97], who examined the sonochemical effects on syntheses of zeolite NaA. Several-fold reductions in nucleation time and rates of formation during hydrothermal synthesis were monitored

References see page 2015

by X-ray diffraction. Scanning electron micrographs showed significant changes in morphology also, with ultrasound producing a more agglomerated product made up of finer, micron-sized crystallites. Delaminated zeolites [98] have also been prepared by exposure to ultrasound, resulting in disordered, individual sheets of crystalline zeolitic materials; the delaminated zeolites were compared with conventional zeolites for a variety of acid-catalyzed organic reactions and found to have superior catalytic activity.

8.5.2.5 Supported Catalysts

The use of ultrasound in the preparation of supported metal catalysts has been examined primarily for hydrogenation reactions. For example, ultrasonic irradiation during the deposition of Pt on silica produces an 80% increase in Pt dispersion [99]. UV–visible, pH and transmission electron microscopy measurements have been conducted on supported catalysts prepared in the presence of ultrasound [100]; these studies indicated that the enhanced dispersion is probably due to a faster rate of metal reduction due to radical production from the sonolysis of water or other solvent molecules. Under appropriate conditions, it is believed that ultrasound can assist the insertion of metal particles into support pores due to microjet and/or shockwave formation accelerating metal agglomerates into the support material [101]. Several Japanese patents make use of ultrasound to improve the dispersion and reliability of supported noble metal for fuel cells [102, 103]. The general process described involves the reduction of H_2PtCl_6 in a carbon carrier, often colloidal, in the presence of ultrasonic irradiation.

Ultrasound can also alter the reactivity of already formed supported catalysts. Han and coworkers examined the acceleration of hydrosilation reactions of alkenes and alkynes catalyzed by Pt/C in the presence of ultrasound [104, 105]. Various substrates, including 1-hexene, styrene and phenylacetylene, work effectively even at $-30\,^{\circ}C$ with various silanes. The separation of products from catalyst by filtration, however, is not possible as ultrasonic treatment generates a fine colloidal suspension of support material, thus defeating one of the primary advantages of heterogeneous catalysis. These researchers extended the use of this system to the hydrogenation of alkenes using formic acid as a hydrogen transfer agent and Pd/C catalyst [106]. In this case, filtration was still effective for removal of the catalyst, but rate enhancements were no greater than with heating. Replacing formic acid with hydrazine yielded similar results [107].

Török and coworkers have developed highly chemoselective and enantioselective hydrogenation catalysts that incorporate a sonochemical pretreatment to supported Pt and Pd catalysts [108, 109]. For example, a two-fold increase in the rate of hydrogenation of cinnamaldehyde was observed for Pt/SiO_2 catalysts treated with ultrasound [108]; the selectivity for cinnamyl alcohol increased by 45%. A similar rate enhancement was observed for the hydrogenation of prochiral carbonyl compounds to their corresponding (*R*)-hydroxyl derivatives [110]. The addition of cinchonidine, a chiral modifier, to the pretreatment solution, increased enantioselectivity for a Pt/Al_2O_3 catalyst with various substrates including ethyl pyruvate (97% *ee*), methyl pyruvate (95% *ee*), ethyl 4-phenyl-2-oxobutyrate (95% *ee*) and ethyl benzoylformate (92% *ee*). These are the best *ees* ever achieved for this heterogeneous system; these results are probably due to more effective surface modification achieved with ultrasonic pretreatment.

The influence of ultrasound on supported catalyst preparation has been extended beyond noble metal deposition by Suslick's group. A nanostructured, bifunctional catalyst, Mo_2C/ZSM-5, was prepared by irradiation of $Mo(CO)_6$ and HZSM-5 in a slurry with hexadecane [111]. As the event responsible for the formation of metal clusters is in the gas phase of the collapsing bubbles and therefore separate from the oxide support, eggshell catalysts are formed; ~2-nm Mo_2C particles decorate the surface of the ZSM-5 support. Studies of the dehydroaromatization of methane to benzene were performed.

Several supported HDS catalysts have been prepared using ultrasound. Suslick and coworkers [112] prepared Co- and Ni-promoted MoS_2 supported on alumina through high-intensity ultrasonic irradiation of isodurene slurries containing $Mo(CO)_6$, $Co_2(CO)_8$, elemental sulfur and Al_2O_3 or $Ni-Al_2O_3$ under an Ar flow. The sonochemically prepared catalysts are extremely active catalysts for the HDS of thiophene and dibenzothiophene with activities several times those of comparable catalysts under identical conditions. Moon's group has also prepared MoS_2/Al_2O_3 [113]. Through the use of ultrasound, higher loadings of Mo can be achieved, resulting in a more active catalyst. A $CoMoS/Al_2O_3$ catalyst has also been prepared by combining sonochemical and CVD techniques [114].

The effect of ultrasound on the gas–solid heterogeneous catalytic decomposition of cumene to benzene and propylene was examined with a silica–alumina cracking catalyst where the entire reaction bed was subjected to ultrasound [115]. Rate improvements of up to 160% were observed. Because cavitation cannot occur in such a system, these results must come simply from improved mass transport between the gas and surface.

Loss of activity during extensive use is a common industrial problem with any catalyst, but especially with supported metal catalysts. The deactivation process varies depending on the catalyst and conditions of use and includes coking, oxidation of metal surfaces and neutralization of surface acid sites. There is an extensive patent literature over the past 20 years describing the use

of ultrasound to regenerate spent catalysts. Although the mechanism of action has not been examined, it is likely that improved mass transport and increased fine-pore penetration are significant contributors. The selectivities of these systems were greatly enhanced.

An early disclosure of the use of ultrasound to reactivate a deactivated hydrocarbon conversion catalyst goes back to Exxon Research and Engineering in 1978 [116]. Highly deactivated hydrocracking catalysts could be reclaimed by oxidizing the catalyst at elevated temperatures followed by ultrasonic irradiation of the catalyst in a non-reactive liquid.

A variety of similar applications of ultrasound to clean or reactivate various catalysts have also been reported. The most common carrier/cleaning liquid phase has been either aqueous [117] or standard feedstock flow. Commercial noble metal catalysts supported on alumina used either for NO_x removal or hydrogenation of hydrocarbons have been regenerated efficiently with ultrasound [118, 119] with nearly complete restoration of specific surface area, porosity and activity. In the same manner, substantial regeneration has been disclosed for deactivated $TiO_2-V_2O_5$ catalysts for oxidation of *o*-xylene to phthalic anhydride [120] and for flue gas denitration [121]. Ultrasonic reactivation is also useful for a partially deactivated BF_3–graphite intercalate catalyst used in an alkylation process [122].

8.5.2.6 Polymerization Catalysts

Ultrasound is commonly used to accelerate rates of polymerization or to modify the structure of existing polymers [5, 123]. There are, however, only a few examples of the use of ultrasound to modify heterogeneous catalysts for polymerization. The first was in a 1961 patent [124], which found a substantial decrease in catalyst particle size and a consequent increase in activity due to diminished aggregation of Ziegler–Natta catalysts [125]. Further investigations of Ziegler–Natta polymerization under high-intensity ultrasound of styrene using a $TiCl_4-Et_3Al$ catalyst have been published [126, 127]. The polymers are produced in better yield and with more control over the molecular weight distribution than in the conventional, unsonicated process. For example, polystyrene produced under the same conditions as stirring yields polydispersities above 10, whereas with ultrasound they are 2.5, with comparable mean molecular weights of ~50 000. In part, this may be due to preferential cleavage of the longer chains by the ultrasound [128].

8.5.3 Conclusion

In principal, ultrasound is well suited to industrial applications. Since the reaction liquid itself carries the sound, there is no barrier to its use with large volumes. In fact, ultrasound is already heavily used industrially for the physical processing of liquids, such as emulsification, solvent degassing, solid dispersion and sol formation. It is also extremely important in solids processing, including cutting, welding, cleaning and precipitation. Ultrasonic spray pyrolysis (USP), an aerosol synthesis technique, is also commonly used in industry for the production of fine powders. Recently, USP has been used to generate catalytic materials [129], although cavitation plays no role in such syntheses other than contributing to the formation of the liquid aerosol.

Ultrasound has already become a common laboratory tool for nearly any case where a liquid and a solid must react. The production of heterogeneous catalysts involves high value-added materials, where processing costs are not always economically limiting. In this context, ultrasound is a viable method for the preparation and treatment of heterogeneous catalysts. The ability of ultrasound to create highly reactive surfaces, to improve mixing even in viscous media and to increase mass transport makes it a particularly promising technique to explore for catalyst preparation, activation and regeneration.

References

1. L. A. Crum, T. J. Mason, J. Reisse, K. S. Suslick (Eds.), *Sonochemistry and Sonoluminescence*, NATO ASI Series C, Vol. 524, Kluwer, Dordrecht, 1999, p. 424.
2. K. S. Suslick (Ed.), *Ultrasound: Its Chemical, Physical and Biological Effects*, VCH, New York, 1988, p. 336.
3. T. J. Mason (Ed.), *Advances in Sonochemistry*, Vols. 1–6, Elsevier, New York, 1990–2001.
4. T. J. Mason, J. P. Lorimer, *Applied Sonochemistry*, Wiley-VCH: Weinheim, 2002, p. 314.
5. K. S. Suslick, G. Price, *Annu. Rev. Mater. Sci.* **1999**, *29*, 295–326.
6. K. S. Suslick, D. A. Hammerton, R. E. Cline Jr., *J. Am. Chem. Soc.* **1986**, *108*, 5641–5642.
7. E. B. Flint, K. S. Suslick, *Science* **1991**, *253*, 1397–1399.
8. K. S. Suslick, K. A. Kemper, in *Bubble Dynamics and Interface Phenomena*, J. R. Blake, N. Thomas (Eds.), Kluwer, Dordrecht, 1994, pp. 311–320.
9. W. B. McNamara III, Y. Didenko, K. S. Suslick, *Nature* **1999**, *401*, 772–775.
10. Y. Didenko, W. B. McNamara III, K. S. Suslick, *J. Phys. Chem. A* **1999**, *103*, 10783–10788.
11. W. Lauterborn, H. Bolle, *J. Fluid Mech.* **1975**, *72*, 391–399.
12. C. M. Preece, I. L. Hansson, *Adv. Mech. Phys. Surf.* **1981**, *1*, 199–254.
13. K. S. Suslick, S. J. Doktycz, *Science* **1990**, *247*, 1067–1069.
14. T. Prozorov, R. Prozorov, K. S. Suslick, *J. Am. Chem. Soc.* **2004**, *126*, 13890–13891.
15. K. S. Suslick, S. J. Doktycz, in *Advances in Sonochemistry*, T. J. Mason (Ed.), Vol. 1, JAI Press, New York, 1990, pp. 197–230.
16. K. S. Suslick, M. L. H. Green, M. E. Thompson, K. Chatakondu, *J. Chem. Soc., Chem. Commun.* **1987**, 900–901.

17. J. Lindley, T. J. Mason, J. P. Lorimer, *Ultrasonics*, **1987**, *25*, 45–58.
18. M. G. Sulman, *Russ. Chem. Rev.* **2000**, *69*, 165–177.
19. A. N. Mal'tsev, *Zh. Fiz. Khim.* **1976**, *50*, 1641–52.
20. K. S. Suslick, *Mod. Synth. Tech.* **1986**, *4*, 1–60.
21. J. L. Luche, *Synthetic Organic Sonochemistry*, Plenum Press, New York, 1998.
22. C. Horst, U. Kunz, A. Rosenplänter, U. Hoffman, *Chem. Eng. Sci.* **1999**, *54*, 2849–2858.
23. J. L. Luche, *Ultrasonics* **1992**, *30*, 156–162.
24. K. S. Suslick, D. J. Casadonte, *J. Am. Chem. Soc.* **1987**, *109*, 3459–3461.
25. K. S. Suslick, S. J. Doktycz, *J. Am. Chem. Soc.* **1989**, *111*, 2342–2344.
26. K. S. Suslick, S. J. Doktycz, *Chem. Mater.* **1989**, *1*, 6–8.
27. A. V. Romenskii, E. N. Mostovaya, *Khim. Prom. Ukr. (Kiev)* **2005**, 50–52.
28. H. B. Wierner, P. W. Young, *J. Appl. Chem.* **1958**, 336.
29. G. Saracco, F. Arzano, *Chim. Ind.* **1968**, *50*, 314–318.
30. K. J. Moulton Sr., S. Koritala, K. Warner, E. N. Frankel, *J. Am. Oil Chem. Soc.* **1987**, *64*, 542–547.
31. M. Tashiro, M. Nakayama, H. Nakamura, Y. Aoki, A. Takigawa, K. Maeda, I. Tago, M. Yoshida, Jpn. Kokai Tokkyo Koho, Japanese Patent 61 053 228, 1986.
32. E. A. Cioffi, W. S. Willis, S. L. Suib, *Langmuir*, **1988**, *4*, 697–702.
33. E. A. Cioffi, W. S. Willis, S. L. Suib, *Langmuir*, **1990**, *6*, 404–409.
34. A. Tai, T. Kikukawa, T. Sugimura, Y. Inoue, T. Osawa, S. Fujii, *J. Chem. Soc., Chem. Commun.* **1991**, 795–796.
35. H. Li, Q. Meng, M. Wang, Faming Zhuanli Shenquing Gongkai Shuomingshu, Chinese Patent 1 565 731, 2005.
36. J. Mikkola, T. Salmi, *Chem. Eng. Sci.* **1999**, *54*, 1583–1588.
37. J., Mikkola, T. Salmi, R. Sjoholm, P. Maki-Arvela, H. Vainio, *Stud. Surf. Sci. Catal.* **2000**, *130C* (International Congress on Catalysis), 22027–22032.
38. P. Boudjouk, *Comments Inorg. Chem.* **1990**, *9*, 123–148.
39. P. D. Boudjouk, European Patent Application EP 306 177, 1989.
40. P. D. Boudjouk, S. Choi, B. J. Hauck, A. B. Rajkumar, *Tetrahedron Lett.* **1998**, *39*, 3951–3952.
41. L. Wen-Zhou, A. N. Mal'tsev, N. I. Kobozev, *Zh. Fiz. Khim.* **1964**, *38*, 80–88.
42. Y. Masuyama, A. Hayakawa, Y. Kurusu, *J. Chem Soc., Chem. Commun.* **1992**, 1102–1103.
43. J. Ito, M. Sakurai, Jpn. Kokai Tokkyo Koho, Japanese Patent 01 227 360, 1989.
44. H. Itoh, E. Kikuchi, Y. Morita, *Sekiyu Gakkaishi* **1987**, *30*, 324.
45. E. Kikuchi, H. Itoh, *Sekiyu Gakkaishi* **1991**, *34*, 407.
46. B. T. Chang, S. J. Kim, P. B. Hong, *Chem. Lett.* **1989**, 805–808.
47. K. S. Suslick, S. B. Choe, A. A. Cichowlas, M. W. Grinstaff, *Nature* **1991**, *353*, 414–416.
48. M. W. Grinstaff, M. B. Salamon, K. S. Suslick, *Phys. Rev. B* **1993**, *48*, 269–273.
49. R. Bellissent, G. Galli, M. W. Grinstaff, P. Migliardo, K. S. Suslick, *Phys. Rev. B* **1993**, *48*, 15797–15800.
50. K. S. Suslick, T. Hyeon, M. Fang, *Chem. Mater.* **1996**, *8*, 2172–2179.
51. K. S. Suslick, M. Fang, T. Hyeon, A. A. Cichowlas, *Mater. Sci. Eng. A* **1995**, *204*, 186–192.
52. V. Kesavan, P. S. Sivanand, S. Chandrasekaran, Y. Koltypin, A. Gedanken, *Angew. Chem. Int. Ed.* **1999**, *38*, 3521–3523.
53. Y. Mizukoshi, T. Fujimoto, Y. Nagata, R. Oshima, Y. Maeda, *J. Phys. Chem B* **2000**, *104*, 6028–6032.
54. N. A. Dhas, C. P. Raj, A. Gedanken, *Chem. Mater.* **1998**, *10*, 1446–1452.
55. S. C. Emerson, C. F. Coote, H. Boote III, J. C. Tufts, R. LaRocque, W. R. Moser, *Stud. Surf. Sci. Catal.* **1998**, *118*, 773–785.
56. T. S. Popov, D. G. Klisurski, K. I. Ivanov, J. Pesheva, *Stud. Surf. Sci. Catal.* **1987**, *31*, 191.
57. A. V. Romenskii, I. V. Popik, A. Y. Loboiko, V. I. Astroshenko, *Khim. Tekhnol. (Kiev)* **1985**, *3*, 17, 21, 23.
58. S. Bennici, A. Gervasini, M. Lazzarin, V. Ragaini, *Ultrason. Sonochem.* **2005**, *12*, 307–312.
59. E. N. Mokryi, V. L. Starchevskii, *Adv. Sonochem.* **1993**, *3*, 257.
60. D. N. Srivastava, N. Perkas, A. Gedanken, I. Felner, *J. Phys. Chem. B* **2002**, *106*, 1878–1883.
61. D. N. Srivastava, N. Perkas, G. A. Seisenbaeva, Y. Koltypin, V. G. Kessler, A. Gedanken, *Ultrason. Sonochem.* **2003**, *10*, 1–9.
62. N. Perkas, Y. Wang, Y. Koltypin, A. Gedanken, S. Chandrasekaran, *Chem. Commun.* **2001**, 988–989.
63. N. Perkas, Y. Koltypin, O. Palchik, A. Gedankan, S. Chandrasekaran, *Appl. Catal. A* **2001**, *209*, 125–130.
64. N., Perkas, O. Palchik, I. Brukental, I. Nowik, Y. Gofer, Y. Koltypin, A. Gedanken, *J. Phys. Chem. B* **2003**, *107*, 8772–8778.
65. U. R. Pillai, E. Sahle-Demessie, R. S. Varma, *Appl. Catal. A* **2003**, *252*, 1–8.
66. T. Ando, *Adv. Sonochem.* **1991**, *2*, 211.
67. T. Ando, T. Kawate, J. Yamawaki, T. Hanafusa, *Synthesis* **1983**, 637.
68. T. Ando, S. Simm, T. Kawate, J. Ichihara, T. Hanafusa, *J. Chem. Soc., Chem. Commun.* **1984**, 439–440.
69. J. Li, G. Chen, W. Xu, T. Li, *Ultrason. Sonochem.* **2003**, *10*, 115–118.
70. J. Li, W. Xu, G. Chen, T. Li, *Ultrason. Sonochem.* **2005**, *12*, 473–476.
71. S. Wang, J. Li, W. Yang, T. Li, *Ultrason. Sonochem.* **2002**, *9*, 159–161.
72. T. Hanafusa, J. Ichihara, T. Ashida, *Chem. Lett.* **1987**, *4*, 687–690.
73. J. C. Yu, J. Yu, W. Ho, L. Zhang, *Chem. Commun.* **2001**, 242–243.
74. J. C. Yu, L. Zhang, J. Yu, *New J. Chem.* **2002**, *26*, 416–420.
75. J. C. Yu, L. Zhang, J. Yu, *Chem. Mater.* **2002**, *14*, 4647–4653.
76. L. Zhang, J. C. Yu, *Chem. Commun.* **2003**, 2078–2079.
77. L. Davydov, E. P. Reddy, P. France, P. G. Smirniotis, *Appl. Catal. B* **2001**, *32*, 95–105.
78. H. Harada, *Ultrason. Sonochem.* **2001**, *8*, 55–58.
79. T. Hyeon, M. Fang, K. S. Suslick, *J. Am. Chem. Soc.* **1996**, *118*, 5492–5493.
80. J. D. Oxley, M. M. Mdleleni, K. S. Suslick, *Catal. Today* **2004**, *88*, 139–151.
81. S. Li, J. S. Lee, T. Hyeon, K. S. Suslick, *Appl. Catal., A* **1999**, *184*, 1–9.
82. M. M. Mdleleni, T. Hyeon, K. S. Suslick, *J. Am. Chem. Soc.* **1998**, *120*, 6189–6190.
83. K. S. Suslick, N. A. Dhas, unpublished results.
84. N. A. Dhas, K. S. Suslick, *J. Am. Chem. Soc.* **2005**, *127*, 2368–2369.
85. I. Uzcanga, I. Bezverkhyy, P. Afanasiev, C. Scott, M. Vrinat, *Chem. Mater.* **2005**, *17*, 3575–3577.
86. M. Tarasevich, *Ceram. Bull.* **1984**, *63*, 500.

87. E. Blanco, L. Esquivias, R. Litán, M. Piñero, M. Ramírez-del Solar, N. de la Rosa-Fox, *Appl. Organomet. Chem.* **1999**, *13*, 399–418.
88. J. Zarzycki, in *Ultrastruct Processing Advanced Materials*, D. R. Uhlmann, D. R. Ulrich (Eds.), Wiley, New York, 1992, pp. 135–148.
89. N. de la Rosa-Fox, L. Esquivias, M. Pinero, in *Handbook of Organic–Inorganic Hybrid Materials and Nanocomposites*, H. S. Nalwa (Ed.), Vol. 1, American Scientific Publishers, Stevenson Ranch, CA, USA, 2003, pp. 241–270.
90. S. Bernal, J. J. Calvino, M. A. Cauqui, J. M. Rodríguez-Izquierdo, H. Vidal, *Stud. Surf. Sci. Catal.* **1995**, *91*, 461.
91. G. W. Schoenthal, L. H. Slaugh, US Patent 4 730 071, 1988.
92. M. A. Cauqui, J. J. Calvino, G. Cifredo, L. Esquivias, J. M. Rodriguez-Izquierdo, *J. Non-Cryst. Solids* **1992**, *147/148*, 758–763.
93. J. J. Calvino, M. A. Cauqui, G. Cifredo, J. M. Rodríguez-Izquierdo, H. Vidal, *J. Sol–Gel Sci. Technol.* **1994**, *2*, 831–836.
94. N. Tonanon, A. Siyasukh, W. Tanthapanichakon, H. Nishihara, S. R. Mukai, H. Tamon, *Carbon* **2005**, *43*, 525–531.
95. N. Tonanon, A. Siyasukh, Y. Wareenin, T. Charinpanitkul, W. Tanthapanichakoon, H. Nishihara, S. R. Mukai, H. Tamon, *Carbon* **2005**, *43*, 2808–2811.
96. X. Tang, S. Liu, Y. Wang, W. Huang, E. Sominski, O. Palchik, Y. Koltypin, A. Gedanken, *Chem. Commun.* **2000**, 2119–2120.
97. J. Lindley, *Ultrasonics* **1992**, *30*, 163–167.
98. M. J. Climent, A. Corma, V. Fomes, G. Hermenegildo, S. Iborra, J. Miralles, I. Rodriguez, *Stud. Surf. Sci Catal.* **2001**, *135*, 3719–3726.
99. V. I. Shekhobalova, L. V. Voronova, *Vestn. Mosk. Univ., Ser. 2: Khim.* **1986**, *27*, 327.
100. K. Okitsu, A. Yue, S. Tanabe, H. Matsumoto, *Chem. Mater.* **2000**, *12*, 3006–3011.
101. H. Li, R. Wang, Q. Hong, L. Chen, Z. Zhong, Y. Koltypin, J. Calderon-Moreno, A. Gedanken, *Langmuir* **2004**, *20*, 8352–8356.
102. T. Nakamura, Jpn. Kokai Tokkyo Koho, Japanese Patent 63 319 050, 1988.
103. N. Yanagihara, I. Kunio, U. Makoto, T. Mieko, Jpn. Kokai Tokkyo Koho, Japanese Patent 02 051 865, 1990.
104. B. H. Han, P. Boudjouk, *Organometallics* **1983**, *2*, 769–771.
105. D. G. Jang, D. H. Shin, B. H. Han, *J. Korean Chem. Soc.* **1991**, *35*, 745–749.
106. P. Boudjouk, B. H. Han, *J. Catal.* **1983**, *79*, 489–492.
107. D. H. Shin, B. H. Han, *Bull. Korean Chem. Soc.* **1985**, *6*, 247–248.
108. G. Szöllösi, B. Török, G. Szakonyi, I. Kun, M. Bartók, *Appl. Catal. A* **1998**, *172*, 225–232.
109. S. C. Mhadgut, I. Bucsi, M. Török, B. Török, *Chem. Commun.* **2004**, 984–985.
110. B. Török, K. Balázsik, G. Szöllösi, K. Felföldi, M. Bartók, *Chirality* **1999**, *11*, 470–474.
111. G. Dantsin, K. S. Suslick, *J. Am. Chem. Soc.* **2000**, *122*, 5214–5215.
112. N. A. Dhas, A. Ekhtiarzadeh, K. S. Suslick, *J. Am. Chem. Soc.* **2001**, *123*, 8310–8316.
113. J. J. Lee, H. Kim, S. H. Moon, *Appl. Catal. B* **2003**, *41*, 171–180.
114. J. J. Lee, H. Kim, J. H. Koh, A. Jo, S. H. Moon, *Appl. Catal. B* **2005**, *58*, 89–95.
115. W. Lintner, D. Hanesian, *Ultrasonics* **1977**, *15*, 21–26.
116. H. C. Henry, R. Ranganathan, US Patent 4 086 184, 1978.
117. M. Honda, Jpn. Kokai Tokkyo Koho, Japanese Patent 03 000 135, 1991.
118. A. V. Romenskii, A. Y. Loboiko, V. V. Tsimbrovskii, *Khim. Tekhnol. (Kiev)* **1989**, *6*, 94.
119. G. Wachholz, G. Thelen, H. W. Voges, European Patent Application, EP 472 853, 1992.
120. S. Slavov, V. Nikolov, *Geterog. Katal., 5th*(Pt. 1), **1983**, 81–86.
121. Mitsubishi Heavy Industries, Jpn. Kokai Tokkyo Koho, Japanese Patent 58 186 445, 1983.
122. P. G. Rodewald, US Patent 4 914 256, 1990.
123. G. J. Price, *Ultrason. Sonochem.* **1996**, *3*, S229–S238.
124. T. S. Mertes, US Patent 2 968 652, 1962.
125. N. Kobayashi, K. Abe, Jpn. Kokai Tokkyo Koho, Japanese Patent 62 297 302, 1987.
126. G. J. Price, M. R. Daw, N. J. Newcombe, P. F. Smith, *Br. Polym. J.* **1990**, *23*, 63–66.
127. R. C. Hiorns, A. Khoukh, P. Ghigo, S. Prim, J. François, *Polymer* **2002**, *43*, 3365–3369.
128. A. M. Basedow, K. H. Ebert, *Adv. Polym. Sci.* **1977**, *22*, 83–148.
129. S. E. Skrabalak, K. S. Suslick, *J. Am. Chem. Soc.* **2005**, *127*, 9990–9991.